ADVANCES IN ATMOSPHERIC SCIENCES, VOL. 23, NO. 6, 2006, 857–868

A Cloud-resolving Study on the Role of Cumulus Merger in MCS with Heavy Precipitation

FU Danhong*[1,2] (付丹红) and GUO Xueliang[1] (郭学良)

[1] *Laboratory of Cloud-Precipitation Physics and Severe Storms (LACS), Institute of Atmospheric Physics, Chinese Academy of Sciences, Beijing* 100029

[2] *Graduate University of Chinese Academy of Sciences, Beijing* 100039

(Received 13 January 2006; revised 15 May 2006)

ABSTRACT

The cumulus merging processes in generating the mesoscale convective system (MCS) on 23 August 2001 in the Beijing region are studied by using a cloud-resolving mesoscale model of MM5. The results suggest that the merger processes occurred among isolated convective cells formed in high mountain region during southerly moving process play critical role in forming MCS and severe precipitating weather events such as hailfall, heavy rain, downburst and high-frequency lightning in the region. The formation of the MCS experiences multi-scale merging processes from single-cell scale merging to cloud cluster-scale merging, and high core merging. The merger process can apparently alter cloud dynamical and microphysical properties through enhancing both low- and middle-level forcing. Also, lightning flash rates are enhanced by the production of more intense and deeper convective cells by the merger process, especially by which, the more graupel-like ice particles are formed in clouds. The explosive convective development and the late peak lightning flash rate can be found during merging process.

Key words: MM5, MCS, cloud merger, lightning, precipitation

doi: 10.1007/s00376-006-0857-9

1. Introduction

The mesoscale convective system (MCS) is one of the most severe weather phenomena, which brings heavy rain, hail and strong wind. The cumulus merger has an important effect on the formation of MCS and the production of severe weather. Some observations indicate that rainfall increases immediately after the cells merge together (Lopez, 1978; Simpson, 1980), and the role of cumulus merger process has been widely concerned in investigations of development and enhancement of the cloud echo area, mixed-phase microphysics, rainfall and cloud-ground lighting activities (e.g., Simpson et al., 1971, 1980b; Simpson, 1980; Houze and Cheng, 1977; Lopez, 1978; Westcott et al., 1994; Westott and Kennedy, 1989; Keenan et al., 1990; Carey et al., 2000). Simpson et al. (1971) and Simpson (1980) found the merging of two moderate-size cumuli increased a ten-to twenty-fold rainfall, and mergers produce 86% rainfall observed. Recent studies indicate that the average merged convective system is able to produce approximately 30 times more rainfall and mixed-phase ice mass than the mean single-cell system, and the merging process caused a marked increase in the storm updraft size and strength, cloud water, reflectivity structure, tornado intensity, and positive CG lightning production (Carey and Rutledge, 1998; Carey et al., 2000, 2003; Lang and Rutledge, 2002).

Some studies illustrate that storm mergers sometimes occur prior to bow-echo formation (Finley et al., 2001), and thunderstorm mergers were associated with the formation of bow echoes 50%–55% of time by the analysis of the observational data that occurred over the United States from 1996 to 2002 (Kilmowski et al., 2004). Takahashi et al. (2001) illustrated the accelerated growth of graupel and frozen drops near the freezing level during cell merging in Baiu clouds, and very high rain accumulation occurred near the freezing level during cell merging (Takahashi and Shimura, 2004).

Analyses of the observational data show the crucial factor in the cumulus initiating merger process is the low-level convergence produced by cumulus downdraft and their associated cold outflows. Lin and Joyce

*E-mail: fudanhong@mail.iap.ac.cn

(2001) found that the merging of cells were dependent on the rearward speed of cell propagation.

Many numerical simulations show that the primary mechanisms for the occurrence of a cloud merger are pressure gradient and the convergence lifting brought by the downdrafts of cloud nearby, and a pair of clouds merged only with a preferred location of clouds or with windless environment under the influence of environmental wind shear (Orville, 1977; Orville et al., 1980; Turpeinen, 1982; Tao and Simpson, 1984, 1989; Huang et al., 1987a, b; Kogan, 1996). Stalker and Knupp (2003) found the cell separation distance scales as 0.75 times the planetary boundary layer depth for mergers within multicell thunderstorms.

These studies, however, generally adopted idealized methods to initiate convection, which could not objectively reflect the natural cloud merging processes. In addition, the previous studies were primarily conducted in tropical region or in maritime continent, and those focusing on cumulus merger process in continent monsoon climatic region with complex terrain condition are relatively very few. Since the MCS plays a dominant role in producing severe weathers such as downburst, heavy precipitation, and lightning in summer and spring seasons in the Beijing region (Fu and Fu, 2003; Guo and Fu, 2003), the formation mechanism of MCS in the region has not been well understood. This study will focus on the formation of MCS due to cloud merger process by through a mesoscale cloud-resolving model MM5 and to understand how an MCS is formed from single cells by cloud merger.

2. Methodology

Numerical experiments were performed using the 5th generation of the Pennsylvania State University-National Center for Atmospheric Research Mesoscale Model (MM5V3). The initial and boundary conditions data set are constructed from the Global Analyses of the National Center for Environmental Prediction (NCEP) on $1^\circ \times 1^\circ$ resolution. Tri-nested grid domains were used in the current simulation, and domain is centered at 40°N, 116°W. Domain 1 has a resolution of 18 km with 85×85 grid points; Domain 2 has a grid resolution of 6 km with grid points of 85×85; Domain 3 has 2 km grid size and 127×127 grid points. All domains have 23 vertical layers, with sigma level. Grell-scheme of convective parameterization was used for domain 1 and resolved-scale moist processes follow the Schultz-scheme for cloud microphysics. Domain 2 only chooses Schultz microphysics-scheme. Goddard microphysics-scheme was used for domain 3. The parameterization chosen to represent the planetary boundary layer is the Blackadar-scheme and RRTM long-wave-scheme was used. The 25-category US Geological Survey global land-use distribution in MM5 was used with 5-min resolution in domain 1 and 2-min in domain 2 and 30-s in domain 3. The lateral boundary conditions were relaxation/inflow-outflow. The simulation was performed from 0800 23–0800 24 August 2001 (LST, the same hereafter).

3. Results

3.1 *The merger processes observed and simulated*

On 23 August 2001, due to the effect of low vortex system located in the Mongolia region, a large number of convective cells were formed in the northwestern mountainous region of Beijing. Observations from 3830 Doppler Radar, located at the Beijing station, indicate that the convective activity occurred in the afternoon on 23 August 2001 (Fig. 1). These formed single cells gradually merged and eventually formed the MCS. At 1446 LST (Fig. 1a), the echo structure of convective cells had been formed, and the maximum echo reached to about 45 dBZ. But these convective cells had the isolated characteristics with horizontal scale around 10–20 km. By 1538 LST (Fig. 1b), the isolated cells merged and formed several cumulus clusters with different high cores. At the same time, the maximum echo reached to about 50 dBZ and the horizontal scale increased to around 50 km. Hereafter, the clusters continued to develop and intensify, but the area with 50 dBZ decreased due to precipitation. By 1651 LST (Fig. 1c), the merging process of the cumulus clusters happened when they were moving southeastward. The maximum echo was 50 dBZ and the reflectivity of the formed cloud bridge was only about 15 dBZ. By 1925 LST (Fig. 1d), the cumulus clusters have merged together and formed the MCS with several high cores or intensive centers, and the maximum echo was 55 dBZ. During the moving process of the MCS, the merging process of the intensive centers happened. The high precipitation and strong wind took place at this time.

Figure 2 displays the horizontal distribution of the precipitation intensity estimated from Doppler Radar at 1651 LST, and that simulated by model at 1645 LST. It shows that the observed overall precipitation structure is well consistent with that observed. The maximum precipitation intensity of radar reached to about 48 mm h^{-1} while that derived from model exceeds 45 mm h^{-1}. The multi-cores of precipitation are also captured by simulation.

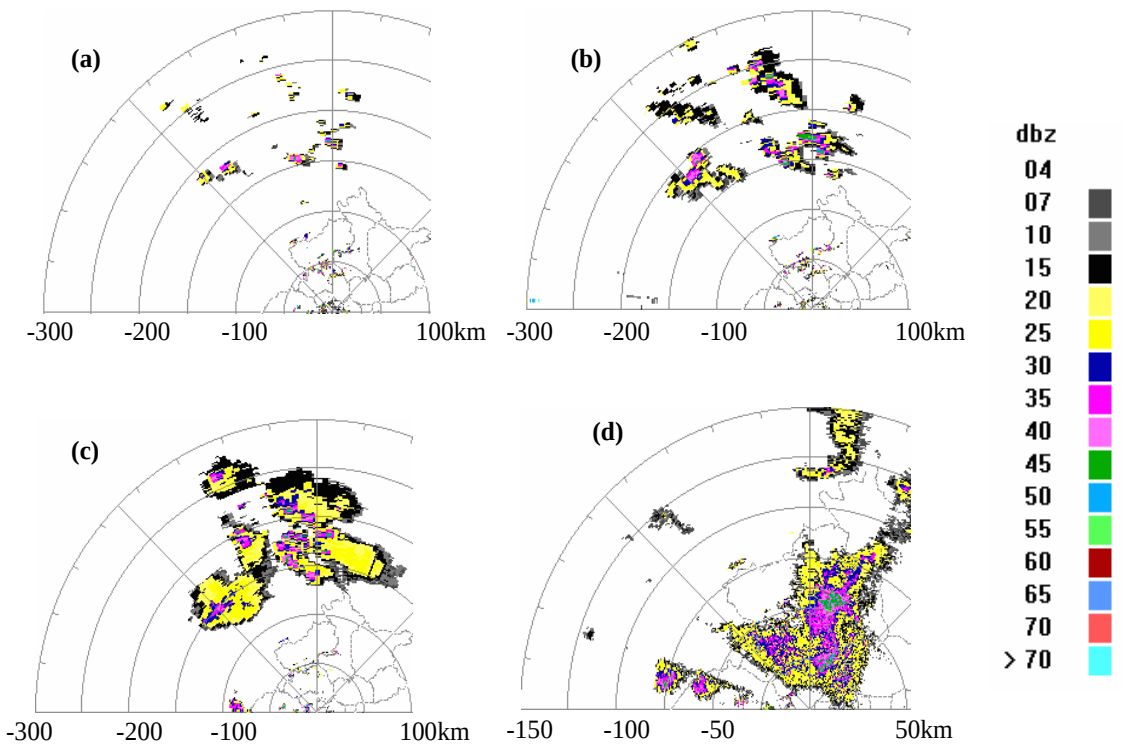

Fig. 1. The horizontal distribution of observational radar reflectivity at an elevation angle of 1.5° on 23 August 2001, (a) 1456, (b) 1538, (c) 1651, and (d) 1925 LST. The detection range of (a), (b) and (c) is 300 km, and that of (d) is 150 km.

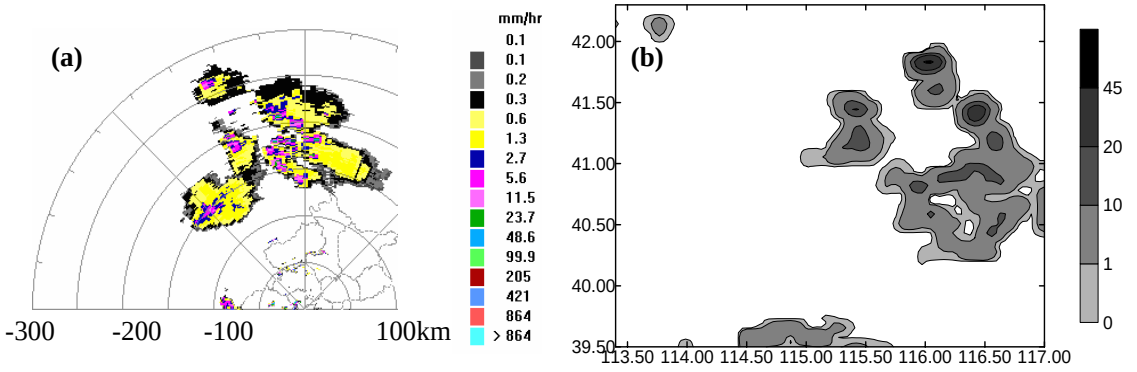

Fig. 2. The horizontal distribution of (a) the estimated precipitation intensity from Doppler Radar at 1651, (b) the simulated precipitation intensity at 1645 LST 23 August 2001.

In order to reproduce the cumulus merger processes in forming the MCS, Fig. 3 displays the time sequences of the simulated radar echo at 500 hPa level. Based on the simulation results, the merging processes can be categorized into three stages: single-cell merging (several to ten kilometers), cloud cluster-scale merging (tens to several hundred kilometers), and high core merging within a MCS. At 1400 LST (Fig. 3a), all cells located in the north mountainous region of Beijing remain isolated and their size is only several ten kilometers, and the maximum echo is around 35 dBZ. These cells move easterly due to the influence of the wind aloft, and by 1415 LST (Fig. 3b) these single cells start to merge and intensify at the same time, and the maximum echo exceeds 45 dBZ. By 1430 LST (Fig. 3c), the main merging processes among single cells have been completed and the relatively small-scale cumulus clusters with several intensive centers are formed. By 1615 LST (Fig. 3d), several previously formed cloud clusters continue to move southeasterly, and to start the second-order merging process among cumulus clusters. In addition, the merging process between cumulus

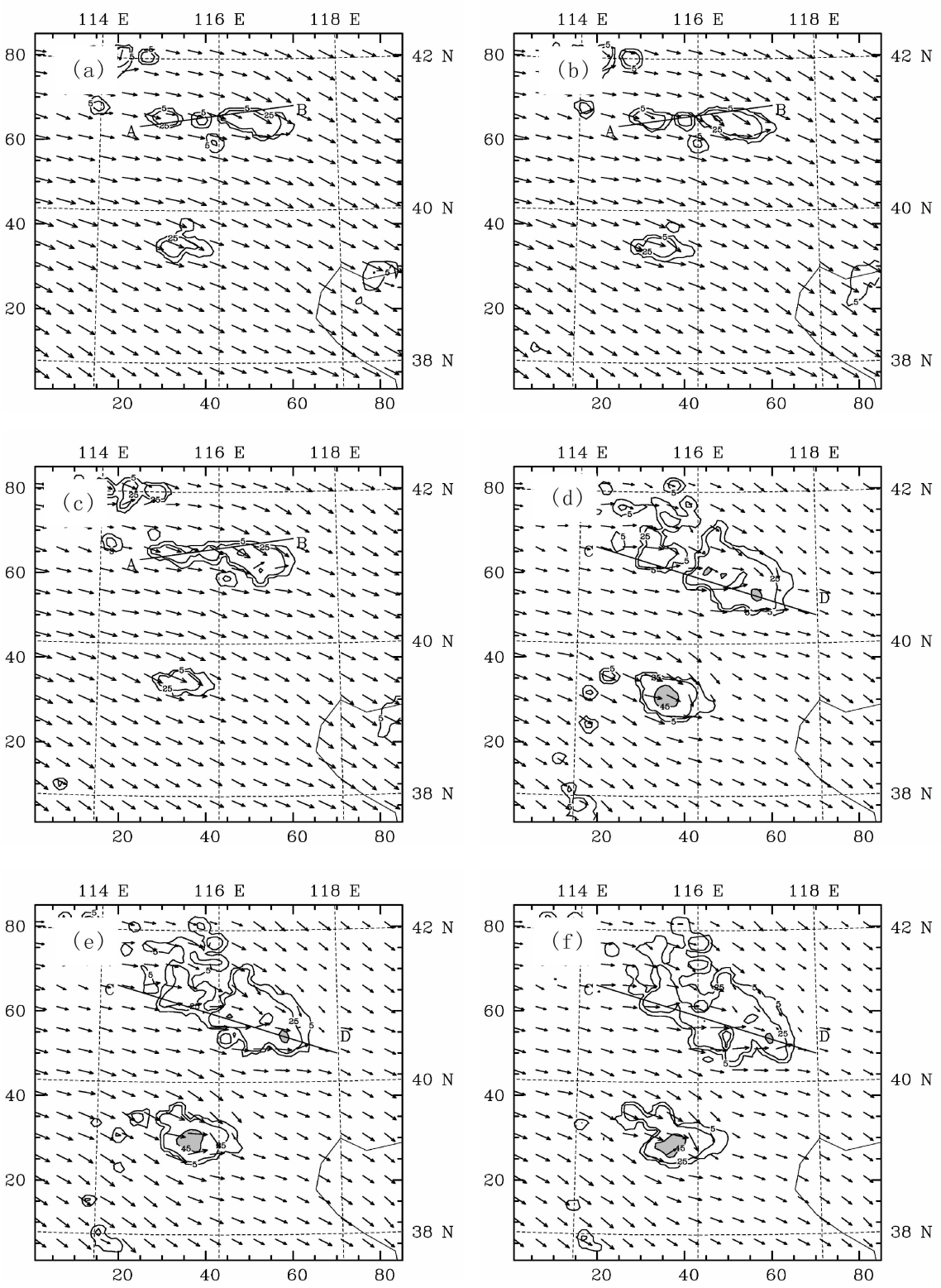

Fig. 3. Time sequence of the simulated radar echo (dBZ) on the 500 hPa of domain 2 and domain 3, respectively (a) 1400; (b) 1415; (c) 1430; (d) 1615; (e) 1630; (f) 1645; (g) 1715; (h) 1730; (i)1745; (j) 1800; (k) 1815; and (l) 1830 LST 23 August 2001.

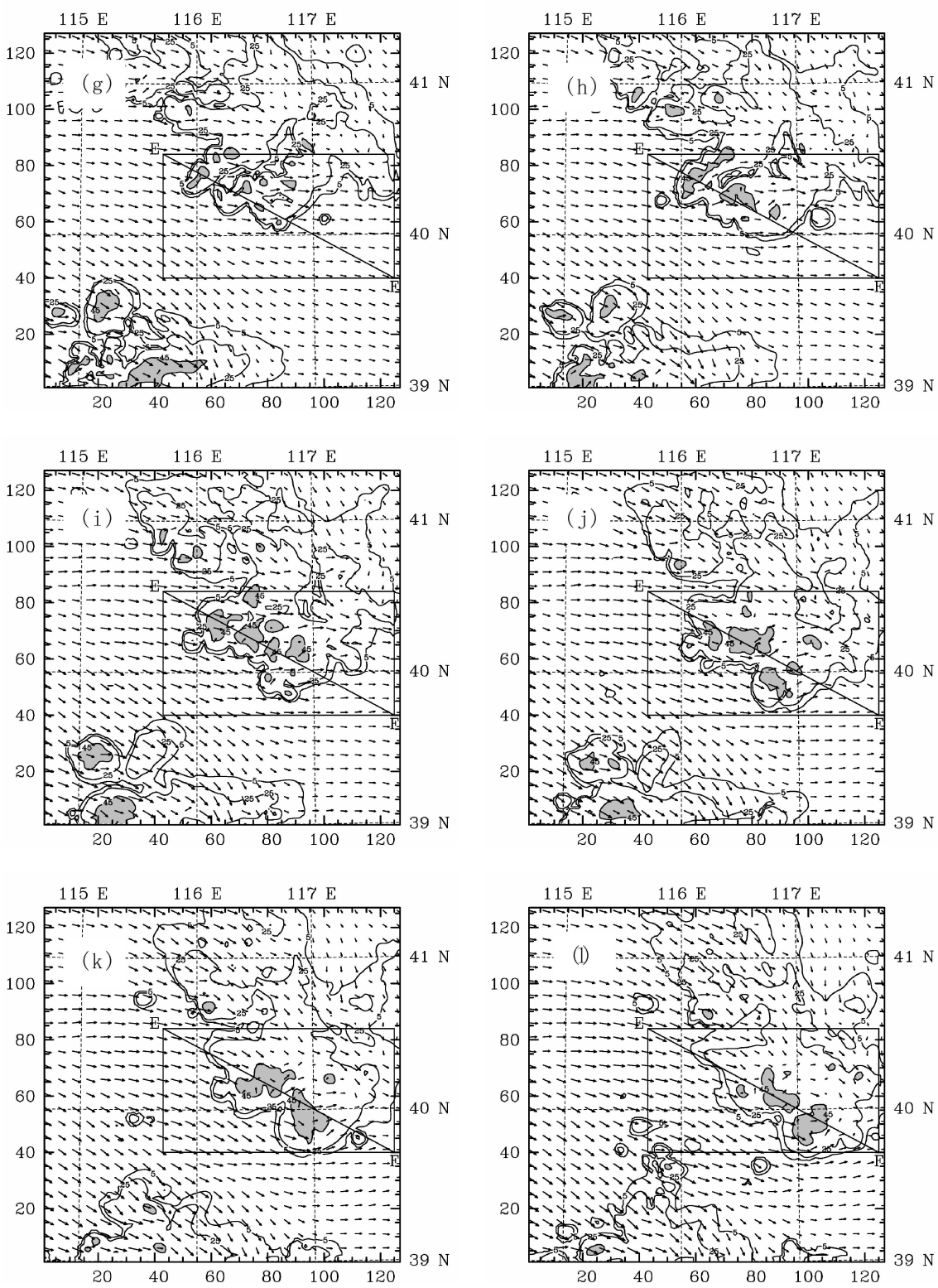

Fig. 3. (Continued).

cluster and single cells also happens at this stage. By 1630 LST (Fig. 3e), three main cumulus clusters begin their merging process. By 1645 LST (Fig. 3f), the individual cumulus clusters almost unite together and form a larger-scale cloud cluster. To clearly show the further merging processes of clusters, radar echo distributions in domain 3 are given in Figs. 3g, h. It shows that cloud cluster-scale merger finally leads to the formation of a mesoscale cloud cluster system. It should be noted that the formed cloud cluster system still has several high cores in this stage, and the merging of these high cores will take place in the next stage.

At 1745 LST (Fig. 3i), there are several high cores or intensive centers exceeded 45 dBZ in this stage. These high cores begin to be combined into several larger-area centers (Fig. 3j), and eventually form two main high cores with 45 dBZ (Figs. 3k, l). The high echo region extends during merging process and forms a line-shape high echo band. Due to the strong precipitation induced by the merging process, the area of the intensive center with 45 dBZ gradually becomes small and the MCS enters a decaying stage.

3.2 *The investigation of merger mechanism*

The results above indicate that the formation of the MCS experiences multi-scale merging processes from single-cell scale to cloud cluster-scale, and then high core merging. Thus, the merger processes are popular in forming the convective cloud system. The questions that in what condition and how the merger process happens are not well understood. To explain the reasons resulting in the merging processes, Fig. 4 shows time evolution of vertical cross sections of the simulated radar echo and wind vector along the lines AB, CD and EF in the Fig. 3. At 1400 LST (Fig. 4a), the cells C_A, C_B and C_C located over the mountainous area remain isolated. The cell C_A is at the initial phase, and the maximum echo locates at above -20°C level where there are a large number of graupel and snow particles. The maximum echoes of cell C_B locate at both above and below -20°C level. There is a strong updraft above the melting level. The cell C_C is at the mature stage, and the maximum echoes locate at both above and below the melting level, and there is a large quantity of ice phase particles at upper levels and high rain water below the melting level. All cells are dominated with updraft. By 1415 LST (Fig. 4b), three cells begin their merging processes. For merging between C_A and C_B, due to the effect of melting and loading of particles, the downdraft formed in the front of C_A intensifies and reaches to the ground to form a strong divergent outflow. The warm and humid air is lifted by the divergent outflow and forms a strong ascending motion. A cloud bridge is formed around the melting level due primarily to the ascending motion. In addition, the horizontal wind component of the tilted downdraft in the front of C_A at the middle levels interacts with the ascending motion to form a stronger wind zone that plays two roles: one is to prohibit the cloud bridge upward development and the other is to enhance the approaching of C_A to C_B. A stronger horizontal wind zone obstructs the upward development of weak updraft, and a large quantity of hydrometeors form at the middle levels. Otherwise the structure of mid-level "jet" provides a favorable condition of the transport of massive particles from C_A to C_B. For the merging of C_B and C_C, the weak downdraft formed below the melting level in the front of C_B interacts with strong updraft in the rear of C_C and forms a cloud bridge. The vorticity calculation shows that there is a strong wind shear (about $2.5\times10^{-4}\,s^{-1}$) in the region between the rear of cell C_C and the front of cell C_B. This shear might enhance the formation of the cloud bridge between cell C_B and C_C at the middle levels. By 1430 LST (Fig. 4c), the cloud bridges between the cells intensify and expand, and unite the separate cells together. With time evolution, the merged cells form cumulus clusters with several intensive centers and with relatively larger scale. By 1615 LST (Fig. 4d), the larger-scale merger processes like those between cumulus clusters and between cumulus cluster and single cell take place. C_D is a cumulus cluster in which the maximum echo locates above -20°C level, and the cloud is dominated by updraft. The airflow ahead C_D is slightly tilted downwards between the melting level and -20°C level due to the effect of downdraft formed within the cell. Though the upper portion of cumulus cluster C_E is merged, it still keeps separate at low levels and has two main high cores in this stage. The airflow structure within C_E reflects an alternately up-down distribution. By 1630 LST (Fig. 4e), the airflow ahead C_D is transformed from partly dominated downdraft to whole downdraft with development of precipitation within the cell. The outflow induced by downdraft lifts air to form a cloud bridge at the middle levels. And also the horizontal wind component formed from the tilted airflow ahead C_D due to interactions of environmental wind with cell downdraft might enhance merging process between C_D and C_E. Some of massive particles resulting from the downdraft transported by this horizontal wind at middle levels, and it has an effect on intensifying the bridge between merging clusters. By 1645 LST (Fig. 4f), except for that at low levels, the merging process between C_D and C_E has almost completed with intensification and

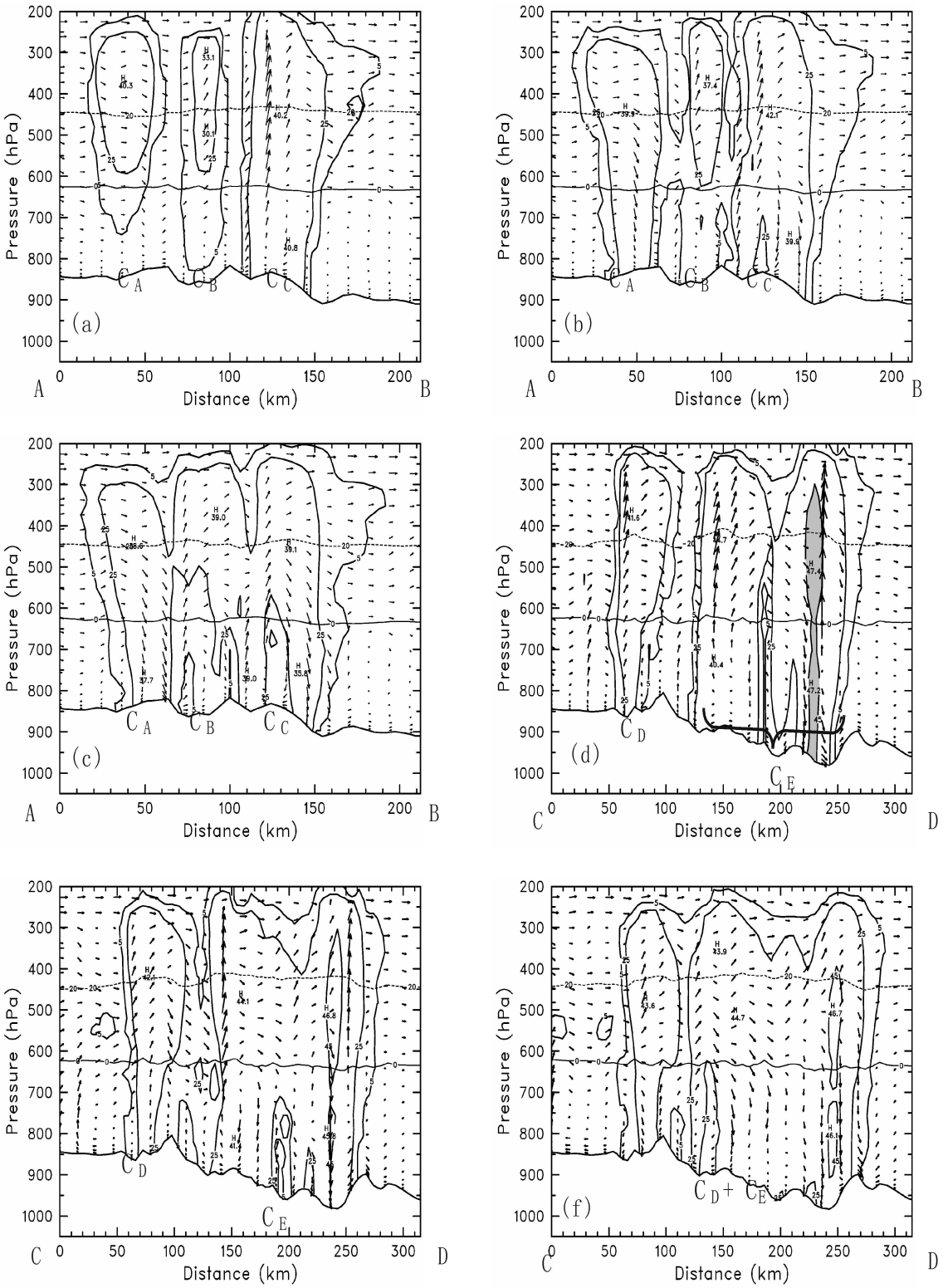

Fig. 4. Time evolution of vertical cross sections of the simulated radar echo (solid lines and shaded area extends 45 dBZ). The 0°C line (horizontally solid) and −20°C line (horizontally dashed) and wind vector along the line AB, CD and EF in the Fig. 3, are also displayed in figures, respectively.

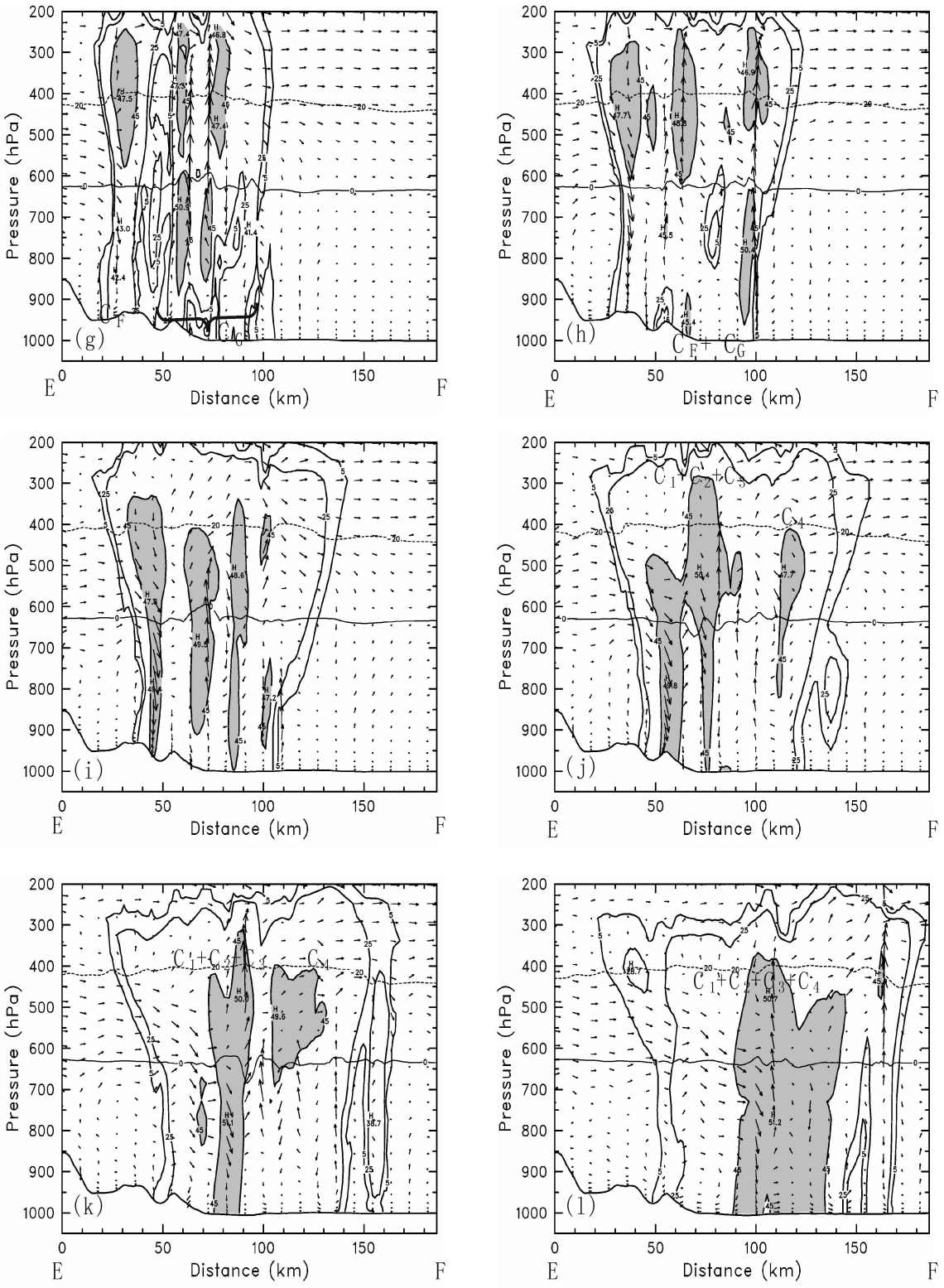

Fig. 4. (Continued).

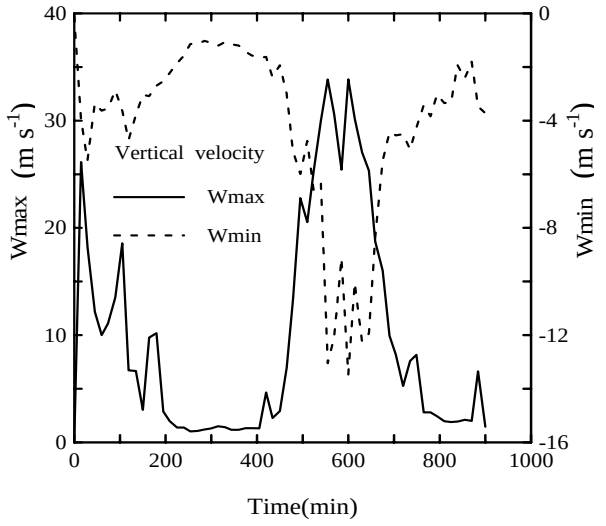

Fig. 5. Time evolution of the maximum updraft and downdraft in the studied region marked with rectangular area.

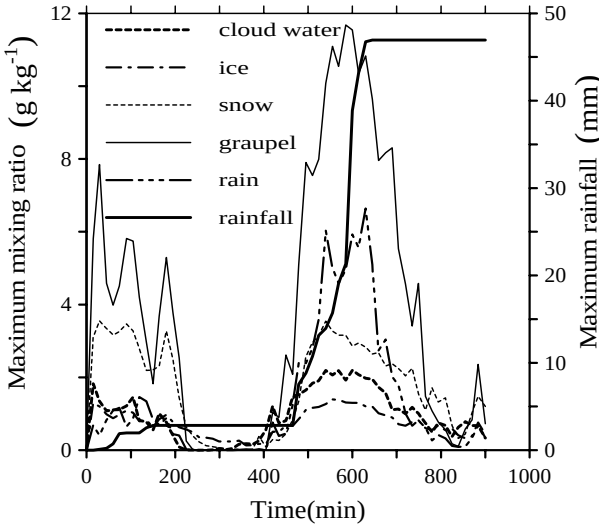

Fig. 6. Time evolution of maximum rainfall and cloud hydrometeors in the studied region marked with rectangular area.

expansion of the cloud bridge. Corresponding to Fig. 3g, h, the vertical cross sections in domain 3 are also shown in Figs. 4g, h and provide more information of merging processes of cloud clusters in the late stage. It shows that the merging occurs at middle levels by forming a cloud bridge. The merging mechanism is consistent with those found in above.

When merging process of cloud cluster is finished, the formed mesoscale cloud system still has several separate cores. By 1745 LST (Fig. 4i), there is an ordered distribution of the updraft and downdraft in the mesoscale convictive cloud system, which corresponds with three intensive centers exceeding 45 dBZ, marked as C_1, C_2 and C_3. C_1 and C_3 are dominated with downdraft while C_2 is dominated with updraft. C_2 is intensified due to the convergence between outflow induced by the strong downdraft of C_1 and the backward outflow of C_3. At the same time, the forward outflow of C_3 forces the lifting of warm air by which the new intensive center C_4 is formed. The updraft induced by the intensified downdraft of C_3 form a cloud bridge between C_3 and C_2 and leads to their merger. By 1800 LST (Fig. 4j), the downdraft generated by the merged C_3 and C_2 interacts with the downdraft formed by C_1 to form another cloud bridge that unites three cells together. C_4 also intensifies at this time.

At 1815 LST (Fig. 4k), the intensive centers C_1 and C_2+C_3 have completed the merging process when C_1 arrives at the plain. In the merged high core, the upper portion of the core is dominated with updraft with maximum echo of 50 dBZ above the melting level while the low-level part of the core is dominated with downdraft with maximum echo of 51 dBZ below the melting level. The ascending motion due to the convergence formed by the interaction of the downdraft of C_1+C_2+C_3 and C_4 is found nearby the melting level. By 1830 LST (Fig. 4l), the merged intensive center C_1+C_2+C_3 combines with C_4 to form an intensive center. The maximum echo reaches to about 50 dBZ and 51 dBZ located at both above and below the melting level respectively, and the cloud top exceeds 45 dBZ. The cold and dry air enters the cloud from its middle and back, and it produces heavy rain and the damaged wind at the surface.

3.3 *The influence of merger process on the cloud dynamical and microphysical structure*

Based on analyses above, cloud merger is primarily induced by downdraft generating from adjacent cells and interactions of the downdraft with environmental airflows. Without any doubt, it is necessary to understand that how the cloud merger processes alter the cloud dynamical and microphysical structure. Figure 5 is time evolution of maximum updraft and downdraft in the studied area marked with a rectangular region. It shows that due to the cloud merger, the maximum updraft and downdraft reach 34 m s^{-1} and -13 m s^{-1}, respectively at 555 min (1715 UTC), and then the updraft and downdraft slightly decrease due to precipitation induced by the merging. By 585 min, during the merging processes of intensive centers, the maximum updraft and downdraft start to intensify again. By 600 min, the maximum updraft and downdraft are 34 m s^{-1} and -13.5 m s^{-1}, respectively, and then gradually decrease. At 615 min, they decrease to 30 m s^{-1} and -10 m s^{-1}, respectively. At 630 min at

which the entire merging of the intensive centers has completed, more precipitation is formed. The maximum updraft decreases to 27 m s^{-1}, while the maximum downdraft increases to -12.3 m s^{-1}. The MCS enters the decaying stage.

Figure 6 shows time evolution of the maximum accumulative rainfall and various hydrometeors. During the merging processes of cloud clusters, cloud water content reaches to the maximum value of 2.18 g kg^{-1} at 570 min. There are large numbers of cloud ice and graupel particles formed in the cloud after cloud cluster merger, and the maximum graupel content reaches to 11.68 g kg^{-1}. But during the high core merging, graupel content decreases while rainwater content increases due to the melting of graupel, the maximum rain water reaches to 6.6 g kg^{-1} at 630 min.

The merger process provides the favorable condition of the transformation of water vapor to cloud hydrometeors. Due to the merger process the cloud water content in the domain reaches the maximum value, and during the high core merger, a large amount of cloud water are transformed to cloud ice and graupel, and the melting of graupel and snow generates rainwater, which yields heavy rain on the ground. The maximum rainfall produced by the merger of the cluster reaches to 21 mm, and the merger of the intensive centers induces the maximum rainfall to quickly increase to 47 mm. More rainfall is yielded by merger processes, in which the intensive center mergers produce much more rainfall than the cumulus cluster mergers.

3.4 *The effect of the merging processes on precipitation intensity and lightning*

It is significant to study the influence of cloud merger on the precipitation intensity and lightning in order to improve predication of disasters produced by severe storms in the region. Figure 7 shows the time evolution of maximum precipitation intensity. At 540 min, the maximum precipitation intensity is 30 mm h^{-1}. By 555 min, the cumulus cluster merger leads to the maximum precipitation intensity reaching to 50 mm h^{-1}. At 600 min, the entirely merged cumulus produces 70 mm h^{-1} of the maximum value. By 645 min, the several intensive centers have been entirely united into one by which the maximum precipitation intensity of 95 mm h^{-1} is reached.

Figure 8 is time evolution of the observational total positive, negative lightning flashes, sampled by Beijing Lightning Detection System (XDD03A) and simulated maximum precipitation intensity. It shows that the occurring time of both negative and positive flashes lags to that of high precipitation intensity. This is perhaps

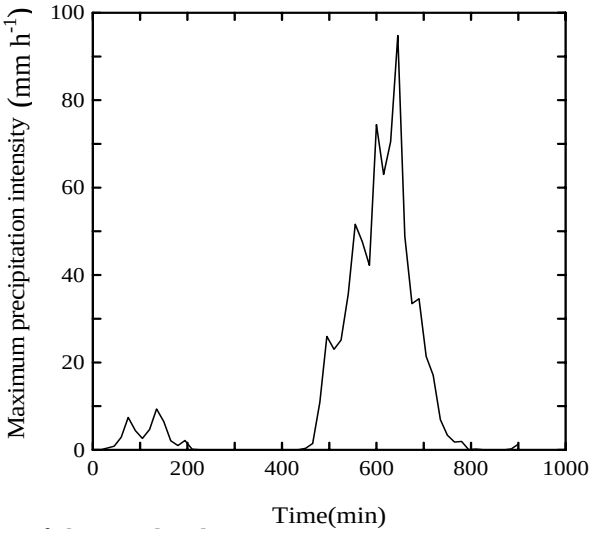

Fig. 7. Time evolution of the simulated maximum precipitation intensity in the studied region marked with rectangular area.

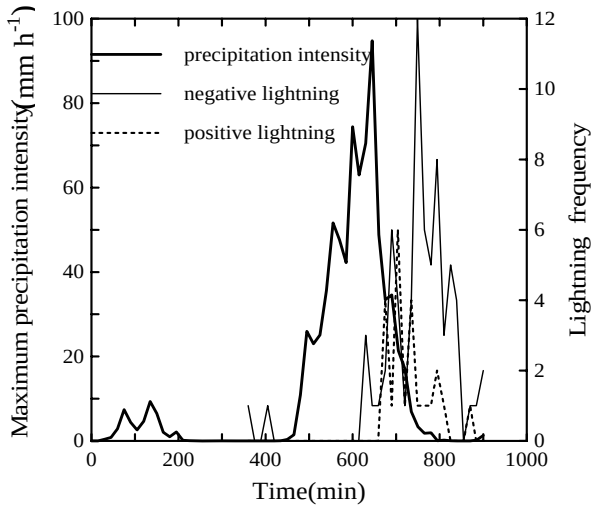

Fig. 8. Time evolution of the observational total lightning flashes and simulated maximum precipitation intensity in the studied region marked with rectangular area.

due to the time difference between the simulated cloud and real cloud, though many field observations also show that lightning is active in the decaying stage of cloud. In addition, the positive flashes keep high value around 700 min at which the disaster wind was produced based on the observation though the negative flashes overwhelmingly dominate lightning activity. According to the formation of cloud hydrometeors, the cloud merger may lead to the rapid increase of supercooled cloud water, cloud ice and graupel content, and to strengthen the precipitation intensity. This process may enhance the negative and positive lightning frequency. When the intensive centers begin to

merge, graupel content rapidly increases and precipitation intensity strengthens, and then the negative lightning reaches the peak. With the merging of the intensive centers, the cloud ice content increases, and positive lightning also reaches its peak. The mergers favor the transforming of water vapor and the forming of cloud ice and graupel and enhance lightning activities. But further study of cloud lightning induced by cloud merger is required.

4. Conclusion

The cumulus merging processes in forming MCS on 23 August 2001 by using a cloud-resolving mesoscale model of MM5 are studied in the paper. The main results can be summarized as follows:

The merger processes are very common in forming a MCS in Beijing area and the multi-scale cloud merging processes from single-cell scale to cloud cluster-scale, and to high core merging are found. The merging process often begins by forming a cloud bridge at the middle levels between two adjacent cells or clusters due to the downdraft generated in the cells or clusters. The interaction of updraft induced by outflows of a cell or cluster with environmental airflow may enhance the merging processes.

The merger processes intensify the up and downdraft, provide the favorable condition of transforming of the water vapor, form a large number of ice phase particles, and produce severe precipitation. Also, lightning flash rates are enhanced by the production of more intense and deeper convective cells by the merger process, especially by which, the more graupel-like ice particles are formed in clouds. The explosive convective development and the late peak lightning flash rate can be found during the merging process.

Acknowledgments. The authors wish to thank Prof. Wu Guoxiong, Chairman of LOC (IAMAS 2005), for inviting us to present this work in the special issue of IAMAS of the International Association of Meteorology and Atmospheric Sciences to be held 2–11 August 2005 in Beijing. This research was jointly sponsored by the Chinese National Natural Science Foundation of China (Grant Nos. 40575003 and 40333033) and the Chinese Academy of Sciences Innovation Foundation (Grant Nos. KZCX3-SW-213 and KZCX3-SW-225), and the Key Project of the Ministry of Science and Technology of China (Grant No. 2001BA610A-06).

REFERENCES

Carey, L. D., and S. A. Rutledge, 1998: Electrical and multiparameter radar case study of the microphysical evolution of a lightning producing storm. *Meteor. Atmos. Phys.*, **59**, 33–64.

Carey, L. D., and S. A. Rutledge, 2000: The relationship between precipitation and lightning in tropical island convection: A c-band polarimetric radar study. *Mon. Wea. Rev.*, **128**, 2687–2710.

Carey, L. D., W. A. Petersen, and S. A. Rutledge, 2003: Evolution of cloud-to-ground lightning and storm structure in the Spencer, south Dakota, tornadic supercell of 30 May 1998. *Mon. Wea. Rev.*, **131**, 1811–1831.

Finley, C. A., W. R. Cotton, and R. A. Pielke Sr., 2001: Numerical simulation of tornadogenesis in high-precipitation supercell. Part I: Storm evolution and transition into a bow echo. *J. Atmos. Sci.*, **58**, 1597–1629.

Fu Danhong, Guo Xueliang, Xiao Wen'an, and Sunlingfeng, 2003: Numerical study on the formation a severe storm accompanied with gale and heavy rain in Beijing. *Journal of Nanjing Institute of Meteorology*, **26**(2), 190–200. (in Chinese)

Guo Xueliang, and Fu Danhong 2003: The formation process and cloud physical characteristics for a typical disastrous wind-producing hailstorm in Beijing. *Chinese Science Bulletin*, **48**(Supp. II), 77–82.

Houze, R. A. Jr., and C.-P Cheng, 1977: Radar characteristics of tropical convection obserbed during GATE: Mean properties and trends over the summer season. *Mon. Wea. Rev.*, **105**, 964–980.

Huang Meiyuan, Xu Huaying, and Ji Wusheng, 1987a: A study on numerical simulation of cloud mergers and interactions. *Science in China*(B), **17**(2), 214–224. (in Chinese)

Huang Meiyuan, Hong Yanchao, Xu Huaying, and Zhou Heng, 1987b: The effects of the existence of stratiform cloud on the development of cumulus cloud and its precipitation. *Acta Meteorologica Sinica*, **45**(1), 72–77. (in Chinese)

Keenan, T. D., B. R. Morton, X. S. Zhang, and K. Nyguen, 1990: Some characteristics of thunderstorms over Bathurst and Melville Islands near Darwin, Australia. *Quart. J. Roy. Meteor. Soc.*, **116**, 1153–1172.

Klimowski, B. A., M. R. Hjelmfelt, and M. J. Bunkers, 2004: Radar observations of the early evolution of bow echoes. *Wea. Forecasting*, **19**, 727–734.

Kogan, Y. L., 1996: The simulation of a convective cloud in 3D model with explicit microphysics. Part II: Dynamical and microphysical aspects of cloud merger. *J. Atmos. Sci.*, **53**(17), 2525–2545.

Lang, T. J., and S. A. Rutledge, 2002: Relationships between convective storm kinematics, precipitation, and lightning. *Mon. Wea. Rev.*, **130**, 2492–2506.

Lin, Y.-L., and L. E. Joyce, 2001: A further study of the mechanisms of cell regeneration, propagation, and development within two-dimensional multicell storms. *J. Atmos. Sci.*, **58**, 2957–2988.

Lopez, R. E., 1978: Internal structure and development processes of C-scale aggregates of cumulus clouds. *Mon. Wea. Rev.*, **106**, 1488–1494.

Orville, H. D., and F. J. Kop, 1977: Numerical simulation of the life history of a hailstorm. *J. Atmos. Sci.*, **34**, 1596–1681.

Orville, H. D., Y- H. Kuo, R. D. Farley, and C. S. Hwang, 1980: Numerical simulation of cloud interactions. *Journal de Recherches Atmospheriques*, **14**, 499–516.

Simpson, J., 1980a: Downdrafts as linkages in dynamic cumulus seeding effects. *J. Appl. Meteor.*, **19**, 477–487.

Simpson, J., W. L. Woodley, A. H. Miller, and G. F.Cotton, 1971: Precipitation results of two randomized pyrotechnic cumulus seeding experiments. *J. Appl. Meteor.*, **10**, 526–544.

Simpson, J., N. E. Westcott, R. J. Clerman, and R. A. Pielke, 1980: On cumulus mergers. *Arch. Meteor. Geophys. Bioklimatol.*, **29**, 1–40.

Stalker, J. R., and K. R. Knupp, 2003: Cell merger potential in multicell thunderstorms of weakly sheared environments: cell separation distance versus planetary boundary layer depth. *Mon. Wea. Rev.*, **131**, 1678–1695.

Takahashi, T., and K. Shimura, 2004: Tropical rain characteristics and microphysics in three-dimensional cloud model. *J. Atmos. Sci.*, **61**, 2817–2845.

Takahashi, T., N. Yamaguchi, and T. Kawano, 2001: Videosonde observation of torrential rain during Baiu season. *Atmospheric Research*, **58**, 205–228.

Tao, W. K., and J. Simpson, 1984: Cloud interactions and merging: Numerical simulations. *J. Atmos. Sci.*, **41**, 2901–2917

Tao, W. K., and J. Simpson, 1989: A further study of cumulus interactions and mergers: Three-dimensional simulations with trajectory analyses. *J. Atmos. Sci.*, **46**, 2947–2957.

Turpeinen, O., 1982: Cloud interactions and merging on day 261 of GATE. *Mon. Wea. Rev.*, **110**, 1238–1254.

Westcott, N. E., 1994: Merging of convective clouds: Cloud initiation, bridging, and subsequent growth. *Mon. Wea. Rev.*, **122**, 780–790.

Westcott, N. E., and P. C. Kennedy, 1989: Cell Development and Merger in an Illinois Thunderstorm Observed by Doppler Radar. *J. Atmos. Sci.*, **46**(1), 117–131.